Nano Progress

Ariviyal Publishing

Research Article

DOI:10.36686/Ariviyal.NP.2019.01.01.005

Nano Prog., (2019) 1(1), 30-36.

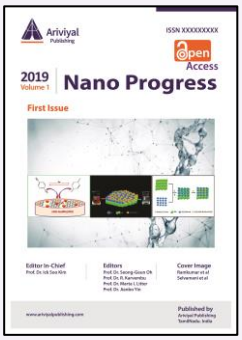

Highly Porous Ru/C and Cu/C Nanocatalysts Derived from Custard Apple for Rapid and Selective Reduction of p-Nitrophenol

Mayakrishnan Gopiraman,[a,b] Muniyandi Muneeswaran[c] and Ick Soo Kim*[a]

[a]*Nano Fusion Technology Research Group, Division of Frontier Fibers, Institute for Fiber Engineering (IFES), Interdisciplinary Cluster for Cutting Edge Research (ICCER), Shinshu University, Tokida 3-15-1, Ueda, Nagano Prefecture 386-8567, Japan*

[b]*Department of Applied Bioscience, College of Life & Environment Science, Konkuk University, 120 Neungdong-ro, Gwangjin-gu, Seoul 05029, South Korea*

[c]*Advanced Materials Laboratory, Mechanical Engineering, University of Chile, Beauchef 851, Santiago, Chile*

***Corresponding author E-mail address**: kim@shinshu-u.ac.jp , kimicksoo.gr@gmail.com (I.S. Kim)

ISSN: 2582-1598

Crossref

Publication details
Received 06th April 2019
Revised 16th May 2019
Accepted 17th May 2019
Published 20th May 2019

Abstract: Nanocatalysts derived from biomass have huge attention due to its positive environmental effects. In the present study, Ru/C and Cu/C nanocatalysts were successfully prepared by using custard apple and metal salts, and the obtained nanocatalysts were employed for the reduction of 4-nitrophenol in water. The Ru/C and Cu/C nanocatalyst were characterized by means of Scanning electron microscope-energy dispersive spectroscope (SEM-EDS), X-ray diffraction (XRD), X-ray photoemission spectroscopy (XPS), Brunauer–Emmett–Teller (BET) and Raman. SEM-EDS spectra of nanocatalysts confirmed the successful loading and wt% of Ru or Cu in nanocatalysts. An excellent BET surface area of 899.15 and 651.78 $cm^2\ g^{-1}$ was determined for the Cu/C and Ru/C, respectively. The presence of defect sites (I_D/I_G ratio) was calculated by Raman analysis. XPS confirmed the chemical state of Cu in Cu/C (+2) and Ru in Ru/C (+4). To our delight, the prepared Cu/C and Ru/C showed superior catalytic activity in 4-nitrophenol reduction reaction. The Ru/C and Cu/C demonstrated an excellent 100% conversion of 4-nitropheonl to 4-aminophenol in very short reaction time. Moreover, it was confirmed that the nanocatalysts are highly active and reusable. It can be reused at least 5 times without significant loss in its yield.

Keywords: Custard apple; Activated carbon; Metal nanoparticles; Nanocomposites; Reduction reaction; Reusability

1. Introduction

Nitrophenols are considered to be major organic pollutants which can be easily found in industrial and agricultural wastewaters.[1, 2] In fact, the nitrophenols are highly soluble in water and stable in soils. The presence of nitrophenols in soil and water often cause harmful effects to human beings, animals and agricultural plants due to its poor degradation, carcinogenesis, hepatotoxicity and mutagenesis. [3] There are several procedures available to recover the nitrophenols from industrial and agricultural wastewaters. The electro-coagulation, electrochemical treatment, adsorption, microwave-assisted catalytic oxidation and microbial degradation methods are highly recommended methods for the removal of nitrophenols.[4] Recently, the conversion of such organic pollutants to valuable compounds has gained huge attention in environmental research. The catalytic reduction of nitrophenols to aminophenols is one of the prime and attractive methods to overcome this issue.[5] In fact the aminophenols are highly useful for the preparation of various compounds such as anticorrosion-lubricant, corrosion inhibitor, photographic developer and analgesic and antipyretic drugs. [6] The reaction is very simple however it can be preceded only in the presence of metal catalysts. The activity of heterogeneous catalysts is highly depends on its physicochemical properties such as surface area and unique morphology. Lv et al.,[7] obtained Pt-Au-pNDs/RGOs catalyst for the reduction of 4-nitrphenol in water. Similarly, Sahoo and co-workers [8] prepared porous Au@Pd@RuNPs catalyst for the reduction of 4-nitrophenol. Similarly, the various heterogeneous catalysts such as Au/PMMA,[9] Ni-RGO,[10] RuDEN,[11] Ag/TiO_2 nanocomposites,[12] Ni@Pd core–shell nanoparticles,[13] NiO/CNP,[14] cellulose nanocomposites,[15] Ag/HHP and Ru/HHP[16] are prepared for the reduction of nitrophenols.

Recently, biomass derived nanomaterials have attracted huge attention due to its environmentally friendly nature and cost-effectiveness. For instance, Veerakumar et al.,[17] prepared highly porous beetroot-derived activated carbons incorporated with well-dispersed magnetite Fe_3O_4 nanoparticles *via* a microwave-assisted synthesis. The prepared magnetic Fe_3O_4@BRAC catalysts were used for the reduction of nitroarenes. Madhu and co-workers [18] employed mango leaves for the preparation of activated carbon and it was used for the electrochemical detection of 4-nitrophenol. In our recent research, we utilized human hair as a catalyst support for the decoration of metal nanoparticles.[19, 20] The metal decorated human hair catalysts Ag/HHP and Ru/HHP were used for the reduction of 4-nitrophenol.[16] In the present study, custard apple was used for the

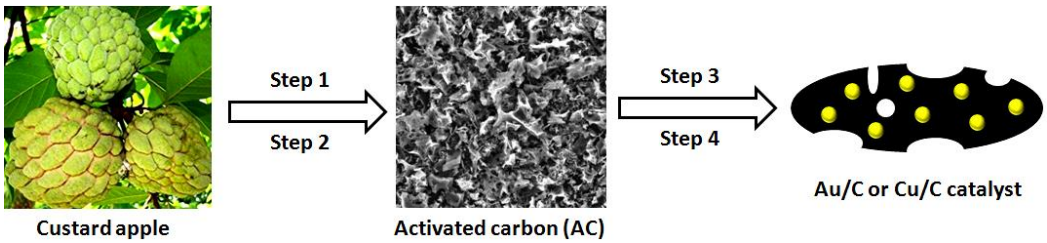

Fig. 1. Schematic illustration for the preparation of Au/C and Cu/C nanocatalysts

preparation of activated carbon and it was employed as catalyst carrier for the incorporating of Ru and Cu nanoparticles. The prepared catalyst Cu/C and Ru/C were characterized by SEM-EDS, Raman, XRD, XPS and BET. Catalytic performance of the Cu/C and Ru/C in the reduction of 4-nitropehnol was investigated. Reusability and reaction kinetics were also investigated in detail.

2. Experimental Section

2.1. Materials and Characterization

Custard apple was collected from shops in Salem, South India. NaOH, HCl, H_2SO_4, and 4-nitophenol were purchased from Wako Pure Chemicals, Japan. Copper(II) acetylacetonate, ruthenium(III) acetylacetonate and $NaBH_4$ were received from Sigma Aldrich, USA. All chemicals were used without any purification and double distilled water was used for the preparation of catalysts and reactions.

Scanning electron microscope-energy dispersive spectroscope (SEM-EDS, Hitachi 3000H SEM), Raman spectra (Hololab 5000, Kaiser Optical Systems Inc., USA) were recorded for Cu/C and Ru/C nanocatalysts. For the Raman analysis, Ar laser was operated at 532 nm with a Kaiser holographic edge filter. X-ray diffraction (XRD, Rotaflex RTP300 (Rigaku Co., Japan) diffractometer) experiment was carried out at room temperature with a scan rate of 2°/min. X-ray photoemission spectroscopy (XPS, Kratos Axis-Ultra DLD, Kratos Analytical Ltd, Japan) was performed for Cu/C and Ru/C. Brunauer–Emmett–Teller (BET) method (BELSORP-max, BEL Japan, Inc.) was adopted to determine the surface area of Cu/C and Ru/C nanocatalysts.

2.2. Preparation of Ru/C and Cu/C

Initially, fresh custard apple skins were cleaned well and dried under sunlight. The dried custard apple skins were pre-carbonized using Muffle furnace under air atmosphere at 250 °C for 1 h (heating rate of 1 °C/min). Then the pre-carbonized sample was mixed with KOH and chemically activated. The KOH: pre-carbonized samples ratio was 2:1. The well mixed KOH/pre-carbonized sample was carbonized at 600 °C under N_2 atmosphere for 2 h. Finally, the samples were washed with dilute HCl solution to obtain activated carbon (AC). The AC was further used to prepare Cu/C and Ru/C nanocatalysts. In a typical preparation method, 25 mg of copper(II) acetylacetonate was add to 250 mg of AC and it was mixed well with mortar and pestle and the mixer was calcinated at 350 °C under N_2 atmosphere for 2 h. Similarly, 25 mg of ruthenium(II) acetylacetonate was add to 250 mg of AC and it was mixed well with mortar and pestle and the mixer was calcinated at 350 °C under N_2 atmosphere for 2 h. Finally, Cu/C and Ru/C was obtained. Fig. 1 shows the schematic illustration for the preparation of Au/C and Cu/C nanocatalysts.

2.3. Catalytic reduction of 4-nitrophenol

In a typical procedure, a mixture of 40 µL of aqueous 4-nitrophenol solution (0.01 M) and 4 mL of fresh $NaBH_4$ solution (0.01 M) was prepared. To the above mixture, 2.5 mg of Cu/C or Ru/C was added and stirred well. The reaction was monitored every 1 min by using UV-Visible spectrometer (Shimadzu UV-2600 spectrophotometer). The UV-Vis absorption spectra were recorded within the wavelength range of 250–600 nm. After the reaction completed, the catalyst was recovered and reused.

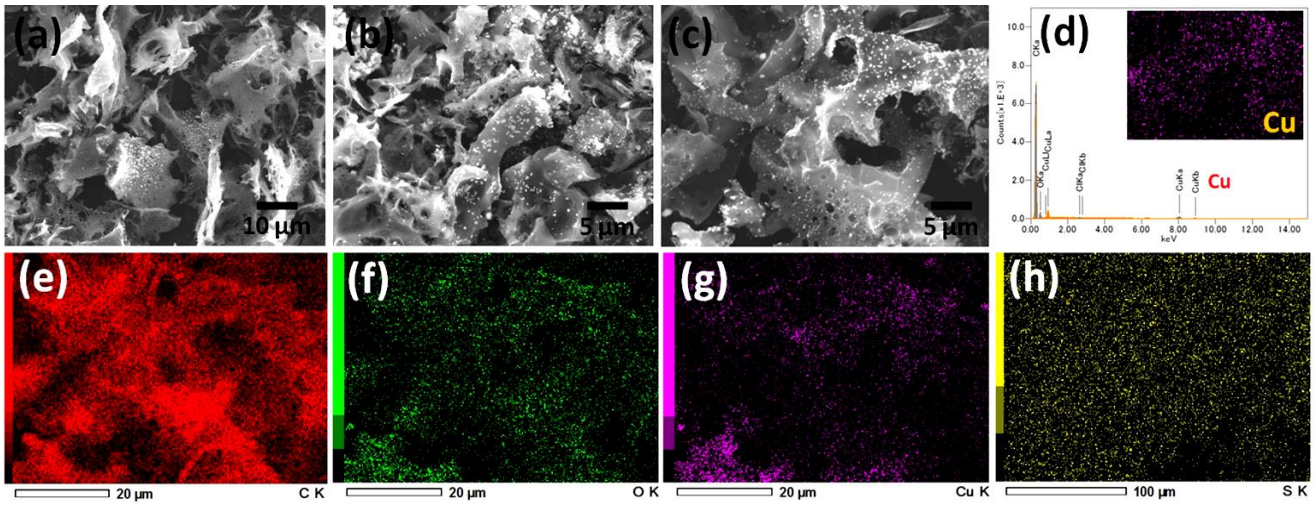

Fig. 2. SEM images (a, b and c), and EDS spectrum (d) of Cu/C, and corresponding elemental mapping of C (e), O (f), Cu (g) and S (h).

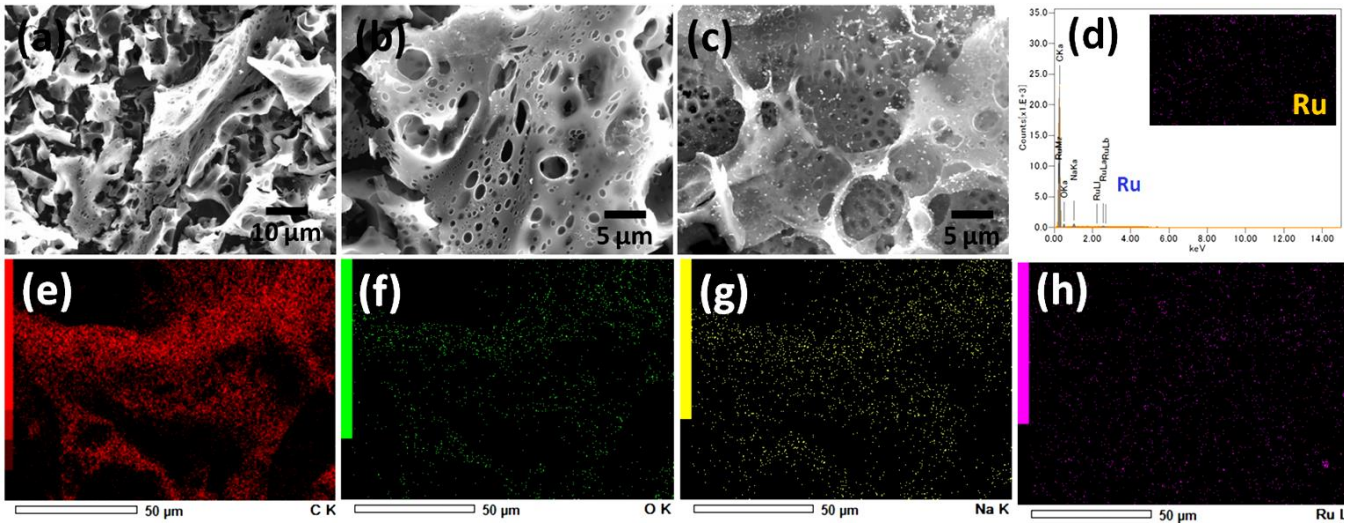

Fig. 3. SEM images (a, b and c), and EDS spectrum (d) of Ru/C, and corresponding elemental mapping of C (e), O (f), Cu (g) and S (h).

3. Results and Discussions

3.1. Characterization of nanocatalysts

The prepared Cu/C and Ru/C were completely characterized by means of various spectral and microscopic techniques. The elements present in the Cu/C and Ru/C were investigated by SEM-EDS (Figs. 2 and 3). SEM images, EDS and corresponding elemental mapping were taken for Cu/C and Ru/C; the results are shown in Figs. 2 and 3. It was confirmed that the chemical activation of custard apple skin successfully produced carbon sheets with several nano/micro/macro holes (Figs. 2 and 3). The diameter of nano-holes was calculated to be 5–75 nm, and the average thickness and holes diameter of carbon nanosheets were 0.5–1 µm and 100–900 nm, respectively. The SEM images of Cu/C and Ru/C showed that the spherical shape of Ru or Cu nanoparticles was strongly attached on the surface of the AC. Moreover, the dispersion of Ru or Cu nanoparticles was observed to be very uniform. The average size of the Ru and Cu nanoparticles was calculated to be 32 and 47 nm respectively. The EDS spectrum of Cu/C confirmed the presence of C, O, S and Cu and its corresponding wt% was 84, 11, 2 and 3, respectively. The Cu elemental mapping showed that the Cu nanoparticles dispersed homogenously on the surface of the AC. Similarly, the Ru/C showed the presence of C (85 wt%), O (11 wt%), Na (1 wt%) and Ru (3 wt%) (Fig.3). The Ru elemental mapping confirmed the uniform decoration of Ru nanoparticles on the surface of AC.

XRD patterns were recorded for the AC, Cu/C and Ru/C nanocatalysts (Fig. 4). A strong characteristic diffraction peak at 22.3° corresponding to (002) and a weak X-ray diffraction peak at around 43.8° corresponding to (101) plane was noticed for all the three samples. The strong X-ray diffraction peak (22.3° corresponding to (002) plane) attributed to a well-defined graphitic stacking and the weak peak at 43.8° indicates to the higher degree of interlayer condensation of carbon.[21] Interestingly, there is no diffraction peaks corresponding to Cu or Ru were noticed either for Cu/C or Ru/C. In addition, no X-ray diffraction peaks corresponding to acetylacetonate groups of Cu $(acac)_2$ or Ru$(acac)_3$ were noticed due to the complete decomposition of metal-$(acac)_3$ to metal nanoparticles. The results confirmed that the Ru and Cu nanoparticles are in nanocrystalline nature.[22] The XRD result aggresses well with the SEM and EDS results.

To further investigate the presence of defect sites in AC, Cu/C and Ru/C, Raman spectra were recorded and the results are provided in Fig.5. The Raman spectra of all AC, Cu/C and Ru/C showed two characteristic bands at 1331 (D band) and 1595 cm^{-1} (G band). The G band represents the graphitic carbon, whereas, the D-band line was related to the amount of disorder.[23] Generally, the I_D/I_G ratio is often calculated to understand the presence of defects and its concentration in carbon matrix.[24] In the present study, the I_D/I_G values were calculated for all the three samples AC, Cu/C and Ru/C. The I_D/I_G values of AC, Cu/C and Ru/C are 0.92, 1.09 and 0.94 respectively. It can be noted that the I_D/I_G values of Cu/C (1.09) and Ru/C (0.94) are high when compared to the I_D/I_G values of AC (0.92). This may be due to the strong interaction of Ru or Cu nanoparticles with the carbon matrix. In fact, the strong interaction of nanoparticles can often create more defect sites in the carbon matrix.[25] The results showed that the Cu/C and Ru/C catalysts have the defect sites.

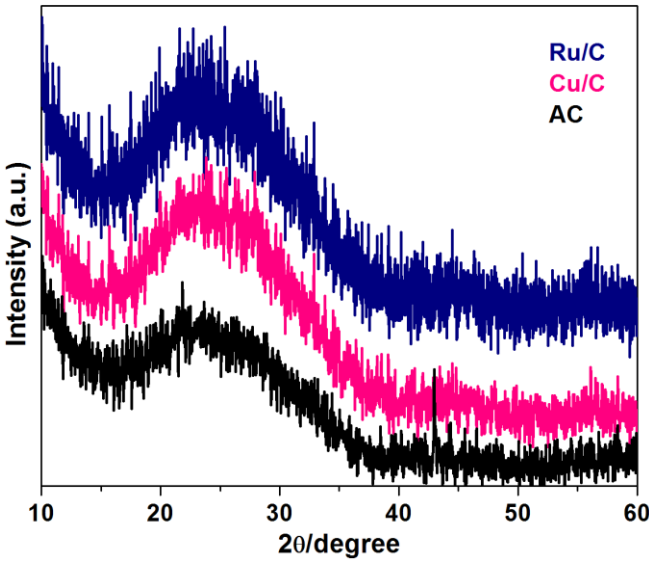

Fig. 4. XRD patterns of AC, Cu/C and Ru/C.

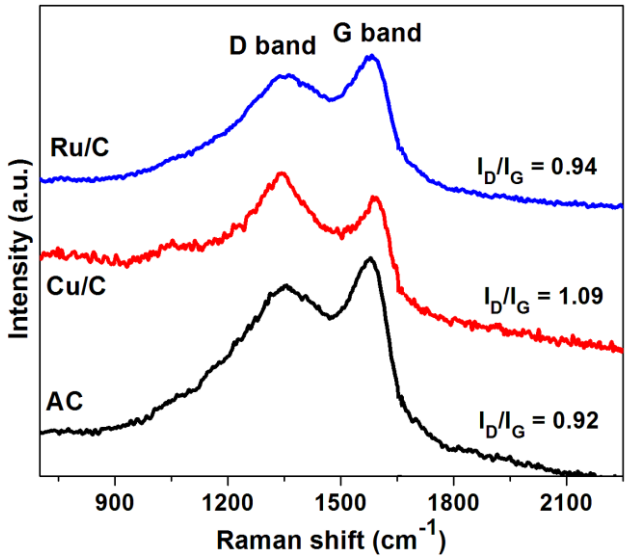

Fig. 5. Raman spectra of AC, Cu/C and Ru/C.

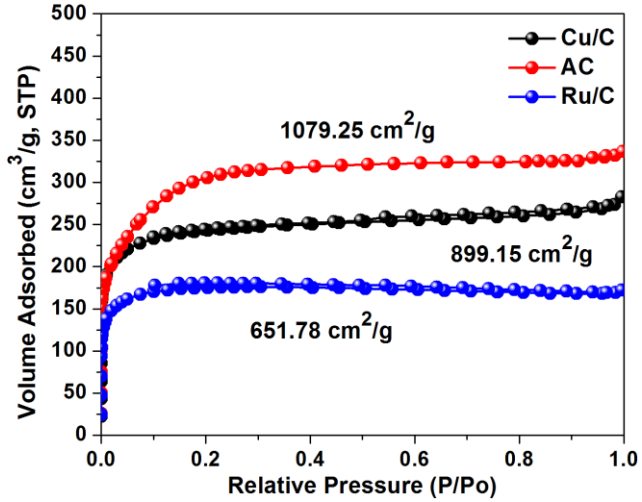

Fig. 6. BET N_2 adsorption isotherms plots of AC, Cu/C and Ru/C.

Fig. 6 shows the N_2 adsorption isotherms of AC, Cu/C and Ru/C. Surface area of the nanocatalyst is often very important since it plays a huge role in any practical applications. Surprisingly, the BET surface area of AC, Cu/C and Ru/C was calculated to be 1079.25, 899.15 and 651.78 cm^2 g^{-1} respectively. In generally, the surface area of carbon materials often shows lower surface area after the decoration of metal nanoparticles which may be due to the blocking of pores and the weight of metal content. Alike, in the present study, the BET surface area of AC showed slightly higher when compared to Cu/C and Ru/C. However, still the nanocatalysts maintained its high the surface area. The results confirmed the presence of well-established microporous in Cu/C and Ru/C. Considering these points, we assumed that the Cu/C and Ru/C would be an efficient catalysts for the reduction of 4-nitrophenol.

In order to investigate the chemical structure, XPS spectra were recorded for AC, Cu/C and Ru/C (Fig. 7). The XPS spectra of all the three samples (AC, Cu/C and Ru/C) demonstrated two intense peaks at ~285 eV (C 1s peak) and ~530 eV (O 1s peak). The strong and sharp C 1s peak at ~285 eV reveal the high graphitic nature of carbon planes.[26] Peak fitting was performed for C 1s and O 1s peaks in order to understand the presence of functional groups in the samples. Fig. 7 shows the decolvolated C 1s and O 1s XPS peaks of AC. Both the C 1s and O 1s peaks were decolvolated into four main peaks corresponding to C–C/C=C, C–OH, C–O–C and C=O functional groups. We presumed that the functional group might have played crucial role for the homogenous dispersion and strong attachment of the Cu or Ru nanoparticles.[27] In fact the oxygen functional groups (C–C/C=C, C–OH, C–O–C and C=O) act as additional anchoring sites for the attachment of nanoparticles. In case of Cu/C, new peaks at binding energy of 934.0 eV (Cu $2p_{3/2}$) and 953.9 eV (Cu $2p_{1/2}$) (with splitting of 19.9 eV) corresponding to CuO was noticed (Fig. 8). In addition, the shake-up satellite peaks at 942.4 (Cu $2p_{3/2}$) and 962.6 eV (Cu $2p_{1/2}$) confirmed the formation of CuO.[28] Similarly, the XPS spectrum of Ru/C showed new peaks in the Ru 3p region (Ru $3p_{3/2}$ at 462.5 eV and Ru $3p_{1/2}$ at 485.2 eV) confirmed the presence of RuO_2.[29]

3.2. Catalytic Performance

After complete characterization, the Cu/C and Ru/C were used as catalysts for the reduction of 4-nitorphenol in water. The reduction reaction was completely monitored by UV-visible spectroscopy. Initially, UV-vis was recovered for aqueous 4-nitrophenol before and after addition of aqueous $NaBH_4$ solution. The typical 4-nitrophenol

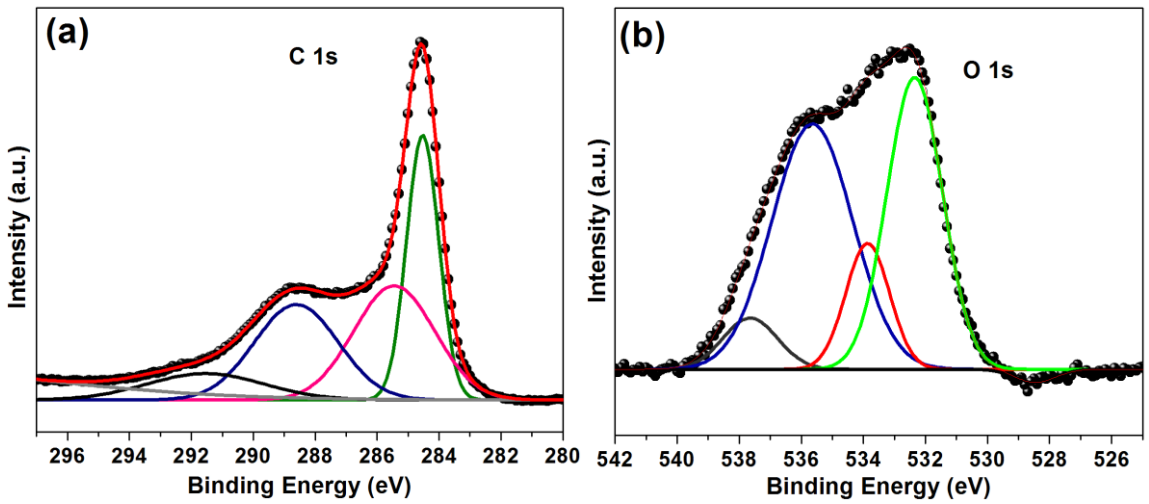

Fig. 7. XPS spectrum of AC; (a) C 1s peak and (b) O 1s peak.

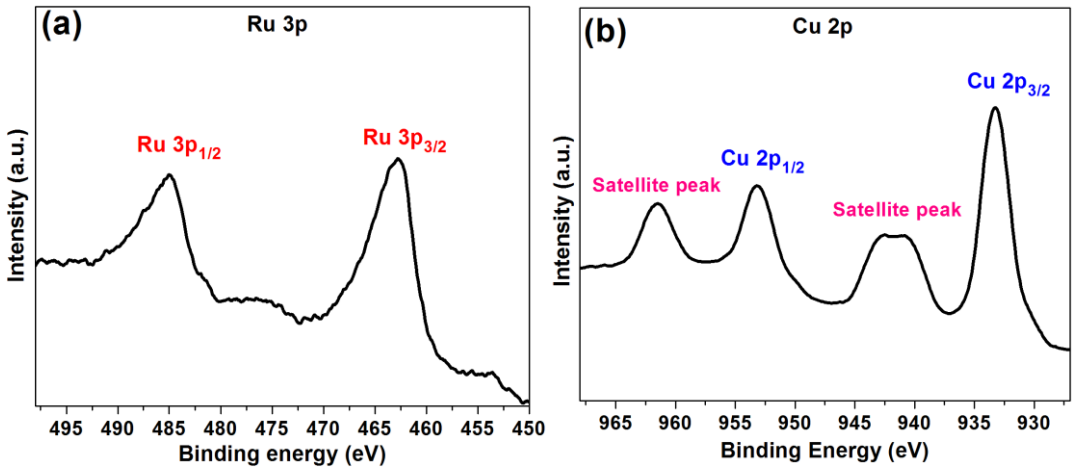

Fig. 8. XPS spectra of (a) Ru 3p peak of Ru/C and (b) Cu 2p peak of Cu/C.

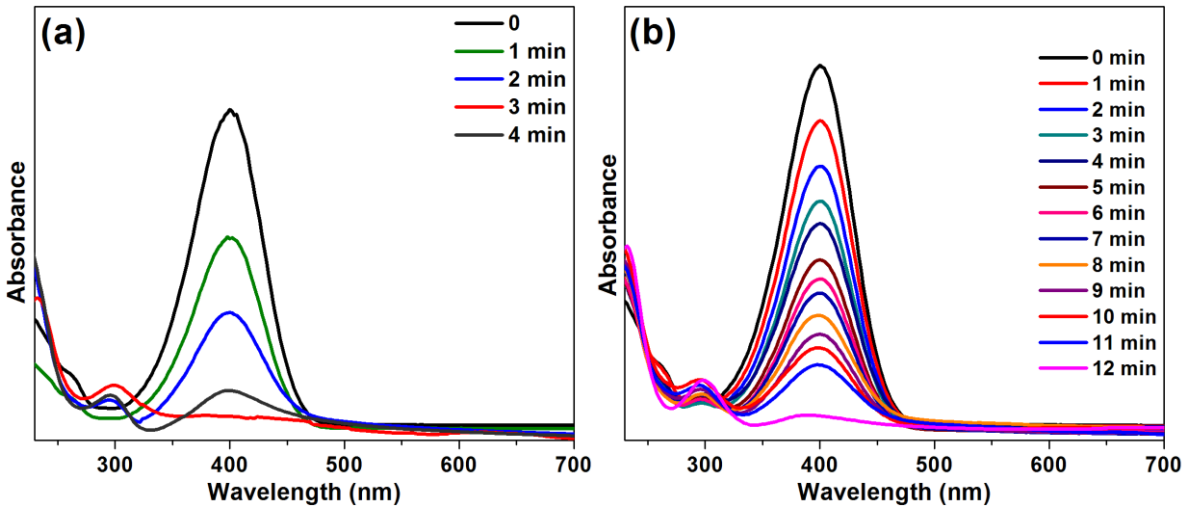

Fig. 9. UV-Vis spectra for the reduction of 4-nitrophenol in aqueous solution recorded every 1 min using (a) Ru/C and (b) Cu/C.

showed absorption band at 314 nm whereas after the addition of $NaBH_4$ the band at 314 nm red-shifted to 400 nm. This is due to the formation of 4-nitrophenolate ion. Fig. 9 shows the UV-Vis spectra for the reduction of 4-nitrophenol in aqueous solution recorded every 1 min using Ru/C and Cu/C. It was confirmed that the fresh AC (without metal content) is not active in the reduction reaction of 4-nitrophenol. A 2 mg of the Cu/C or Ru/C was found to be enough for the complete reduction of 4-nitrophenol to 4-aminophenol. The 4-nitrophenol was completely transferred to 4-aminophenol by 2 mg of Ru/C within 4 min. Similarly, Cu/C gave 100% conversation 4-nitrophenol to 4-aminophenol within 12 min. In comparison to Cu/C, the Ru/C showed better catalytic activity toward the reduction of 4-

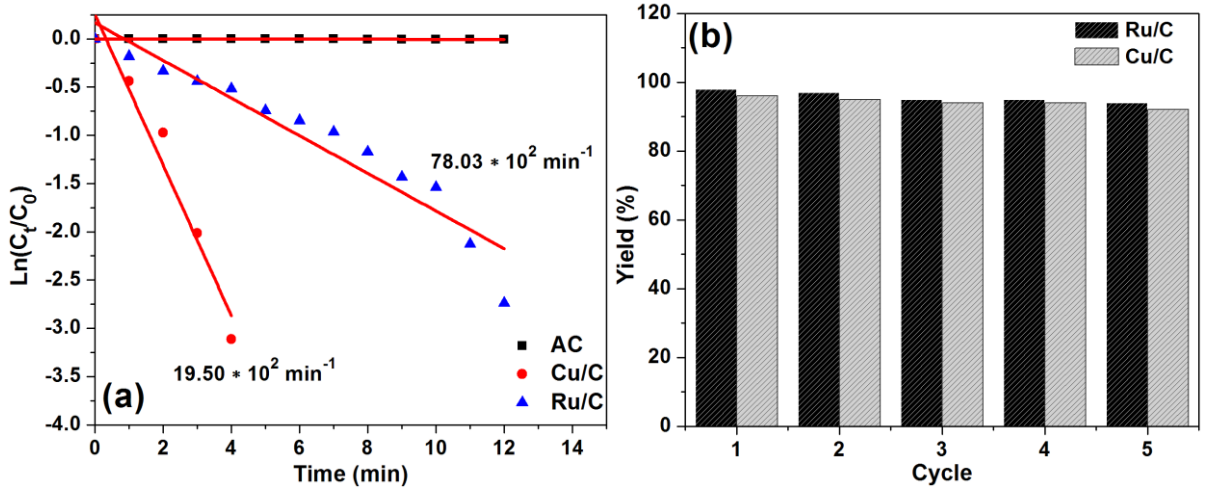

Fig. 10. (a) Plots of $\ln[C_t/C_0]$ *versus* reaction time for the reduction of 4-nitrophenol with $NaBH_4$ over Cu/C and Ru/C, and (b) Reusability of Cu/C and Ru/C.

nitorphenol. The better catalytic of Ru may be due to its wide range of oxidation states (−2 to +8) and tunable properties. In addition, the surface area and small size of Ru nanoparticles are also played an import role in its catalytic activity. Overall, both the Cu/C and Ru/C nanocatalysts are highly activity in the reduction of 4-nitrophenol reaction.

To better understand the catalytic performance of the Cu/C and Ru/C nanocatalysts, reaction kinetics was studied for the 4-nitrophenol reduction reaction by using the time-dependent UV-vis spectra. The use of excess amount of $NaBH_4$ and inactiveness of AC suggest that the rate of reaction is independent of $NaBH_4$ concentration and AC. Linear correlation between ln (C_t/C_0) and time was plotted and rate of reaction (k_{app}) was calculated from the slope of the plots. Fig. 10a shows the Plots of ln [C_t/C_0] *versus* reaction time for the reduction of 4-nitrophenol with $NaBH_4$ over AC, Cu/C and Ru/C. The result confirms that the Cu/C or Ru/C catalyzed reduction reaction of 4-nitrophenol follow the pseudo-first-order reaction kinetics. The rate of the reaction (k_{app}) was calculated to be 78.09 × 10^2 min^{-1} and 19.50 × 10^2 min^{-1} for the reduction of 4-nitropehnol with 2 mg of Ru/C and Cu/C respectively. The values show the excellent catalytic activity of the present catalysts. The k_{app} values of the present system can be compared to the previously reported results. For instance, Lv et al.,[7] prepared Pt-Au-pNDs/RGOs catalyst and used for the reduction of 4-nitrphenol. The k_{app} value of 3.8 × 10^{-3} s^{-1} was calculated for the Pt-Au-pNDs/RGOs catalyzed reduction of 4-nitropehnol reaction. Similarly, Sahoo and co-workers[8] demonstrated porous Au@Pd@RuNPs catalyst for the reduction of 4-nitrophenol and the kapp value was calculated to be 7.20 ± 0.12 × 10^{-3} s^{-1}. Similarly, the present catalytic system can be compared to previously reported catalysts such as Au/PMMA,[9] Ni-RGO,[10] RuDEN,[11] Ag/TiO_2 nanocomposites,[12] Ni@Pd core–shell nanoparticles,[13] NiO/CNP,[14] cellulose nanocomposites,[15] Ag/HHP and Ru/HHP.[16]

3.3. Reusability test

Reusability is one of the very important criteria for the heterogeneous catalysts. In the present study, the reusability test was performed for the Ru/C and Cu/C nanocatalysts. Fig. 10b shows the reusability test of Cu/C and Ru/C towards the reduction of 4-nitrophenol. To our delight, the both the nanocatalysts Ru/C and Cu/C were found to be highly reusable at least for five times without significant loss in its catalytic activity. At 5th cycle, the Ru/C showed 96% conversion of 4-nitrophenol to 4-aminophenol. Similar, at 5th run, the Cu/C gave 93% of 4-aminophenol from the reduction of 4-nitrophenol in the presence of $NaBH_4$. Over all the results confirmed that the Ru/C and Cu/C nanocatalysts are highly active, easy to prepare, green and reusable.

4. Conclusions

In summary, Ru/C and Cu/C nanocatalysts were successfully derived from custard apple by a simple chemical activation followed by metal decoration. Excellent surface morphology, metal loading, and huge BET surface area of Cu/C and Ru/C were confirmed. Raman I_D/I_G ratio confirmed the presence of defect sites in Cu/C and Ru/C. XPS revealed the chemical state of Cu in Cu/C (+2) and Ru in Ru/C (+4). To our delight, the Cu/C and Ru/C demonstrated superior catalysis activity in 4-nitrophenol reduction reaction. An high rate constant k_{app} value of 78.03 and 19.50 × 10^2 min^{-1} was calculated for the reaction of 4-nitrophenol by Ru/C and Cu/C respectively. At 5th cycle, the Ru/C and Cu/C respectively showed 96 and 93% conversion of 4-nitrophenol to 4-aminophenol in the presence of $NaBH_4$. Over all the Ru/C and Cu/C nanocatalysts are found to be highly active, easy to prepare, green and reusable.

Conflicts of Interest

The authors declare no conflict of interest.

References

1 Zhao P.; Feng X.; Huang D.; Yang G.; Astruc D. Basic Concepts and Recent Advances in Nitrophenol Reduction by Gold-and other Transition Metal Nanoparticles. *Coordin. Chem. Rev.,* 2015, **287**, 114-136. [CrossRef]
2 Panigrahi S.; Bas S.; Praharaj S.; Pande S.; Jana S.; Pal A.; Ghosh S.K.; Pal T. Synthesis and Size-Selective Catalysis by Supported Gold Nanoparticles: Study on Heterogeneous and Homogeneous Catalytic Process. *J. Phys. Chem. C*, 2007, **111**, 4596-4605. [CrossRef]
3 Narayanan K.B.; Sakthivel N. Heterogeneous Catalytic Reduction of Anthropogenic Pollutant, 4-nitrophenol by Silver-Bionanocomposite using *Cylindrocladium Floridanum*. *Bioresour. Technol.*, 2011, **102**, 10737-10740. [CrossRef]
4 Chang Y.C.; Chen D.H. Catalytic Reduction of 4-nitrophenol by Magnetically Recoverable Au Nanocatalyst. *J. Hazard Mater.,* 2009, **165**, 664-669. [CrossRef]
5 Sadeghzadeh S.M.; Zhiani R.; Emrani S. The reduction of 4-nitrophenol and 2-nitroaniline by the Incorporation of Ni@ Pd MNPs into Modified UiO-66-NH 2 Metal–Organic Frameworks (MOFs) with Tetrathia-Azacyclopentadecane. *New J. Chem*., 2018, **42**, 988-994. [CrossRef]
6 Mandlimath T.R.; Gopal B. Catalytic Activity of First Row Transition Metal Oxides in the Conversion of p-nitrophenol to p-aminophenol. *J. Mol. Catal. A-Chem*., 2011, **350**, 9-15. [CrossRef]
7 Lv J.J.; Wang A.J.; Ma X.; Xiang R.Y.; Chen J.R.; Feng J.J. One-Pot Synthesis of Porous Pt–Au Nanodendrites Supported on Reduced Graphene Oxide Nanosheets Toward Catalytic Reduction of 4-nitrophenol. *J. Mater. Chem. A*, 2015, **3**, 290-296. [CrossRef]
8 Sahoo A.; Tripathy S.K.; Dehury N.; Patr S. A Porous Trimetallic Au@ Pd@ Ru Nanoparticle System: Synthesis, Characterisation and Efficient Dye Degradation and Removal. *J. Mater. Chem. A*, 2015, **3**, 19376-19383. [CrossRef]
9 Kuroda K.; Ishida T.; Haruta M. Reduction of 4-nitrophenol to 4-Aminophenol over Au Nanoparticles Deposited on PMMA. *J. Mol. Catal. A-Chem*., 2009, **298**, 7-11. [CrossRef]
10 Ji Z.; Shen X.; Zhu G.; Zhou H.; Yuan A. Reduced Graphene Oxide/Nickel Nanocomposites: Facile Synthesis, Magnetic and Catalytic Properties. *J. Mater. Chem. A*, 2012, **22**, 3471-3477. [CrossRef]
11 Antonels N.C.; Meijboom R. Preparation of Well-Defined Dendrimer Encapsulated Ruthenium Nanoparticles and their Evaluation in the Reduction of 4-nitrophenol According to the Langmuir–Hinshelwood Approach. *Langmuir*, 2013, **29**, 13433-13442. [CrossRef]
12 Wang X.; Zhao Z.; Ou D.; Tu B.; Cui D.; Wei X.; Cheng M. Highly active Ag clusters stabilized on TiO_2 nanocrystals for catalytic reduction of p-nitrophenol. *Appl. Surf. Sci*., 2016, **385**, 445-452. [CrossRef]
13 Dong Z.; Le X.; Dong C.; Zhang W.; Li X.; Ma J. Ni@ Pd Core–Shell Nanoparticles Modified Fibrous Silica Nanospheres as Highly Efficient and Recoverable Catalyst for Reduction of 4-nitrophenol and Hydrodechlorination of 4-chlorophenol. *Appl. Catal. B*., 2015, **162**, 372-380. [CrossRef]
14 Somasundaram S.; Ill-Min C.; Vanaraj R.; Ramaganthan B.; Mayakrishnan G. Highly Active and Reducing Agent-Free Preparation

of Cost-Effective NiO-based Carbon Nanocomposite and its Application in Reduction Reactions under Mild Conditions. *J. Ind. Eng. Chem*., 2018, **60**, 91-101. [CrossRef]
15 Gopiraman M.; Deng D.; Saravanamoorthy S.; Chung I.M.; Kim I.S. Gold, Silver and Nickel Nanoparticle Anchored Cellulose Nanofiber Composites as Highly Active catalysts for the Rapid and Selective Reduction of Nitrophenols in Water. *RSC Adv*., 2018, **8**, 3014-3023. [CrossRef]
16 Gopiraman M.; Chung I.M. Multifunctional Human-Hair Nanocomposites for Oxidation of Alcohols, *aza*-Michael Reactions and Reduction of 2-nitrophenol. *J. Korean Chem. Soc*., 2017, **34**, 2169-2179. [CrossRef]
17 Veerakumar P.; Panneer Muthuselvam I.; Hung C.T.; Lin K.C.; Chou F.C.; Liu S.B. Biomass-Derived Activated Carbon Supported Fe_3O_4 Nanoparticles as Recyclable Catalysts for Reduction of Nitroarenes. *ACS Sustain. Chem. Eng*., 2016, **4**, 6772-6782. [CrossRef]
18 Madhu R.; Karuppiah C.; Chen S.M.; Veerakumar P.; Liu S.B. Electrochemical Detection of 4-nitrophenol based on Biomass Derived Activated Carbons. *Anal. Methods*, 2014, **6**, 5274-5280. [CrossRef]
19 Deng D.; Gopiraman M.; Kim S.H.; Chung I.M.; Kim I.S. Human Hair: A Suitable Platform for Catalytic Nanoparticles. *ACS Sustain. Chem. Eng*., 2016, **4**, 5409-5414. [CrossRef]
20 Gopiraman M.; Deng D.; Zhang K.Q.; Kai W.; Chung I.M.; Karvembu R.; Kim I.S. Utilization of Human Hair as a Synergistic Support for Ag, Au, Cu, Ni, and Ru Nanoparticles: Application in Catalysis. *Ind. Eng. Chem. Res*., 2017, **56**, 1926-1939. [CrossRef]
21 Gopiraman M.; Deng D.; Kim B.S.; Chung I.M.; Kim I.S. Three-Dimensional Cheese-like Carbon Nanoarchitecture with Tremendous Surface Area and Pore Construction Derived from Corn as Superior Electrode Materials for Supercapacitors. *Appl. Surf Sci*., 2017, **409**, 52-59. [CrossRef]
22 Gopiraman M.; Ganesh Babu S.; Khatri Z.; Kai W.; Kim Y.A.; Endo M.; Karvembu R.; Kim I.S. Dry Synthesis of Easily Tunable Nano Ruthenium Supported on Graphene: Novel Nanocatalysts for Aerial Oxidation of Alcohols and Transfer Hydrogenation of Ketones. *J. Phys. Chem. C*, 2013, **117**, 23582-23596. [CrossRef]
23 Wu J.B.; Lin M.L.; Cong X.; Liu H.N.; Tan P.H. Raman Spectroscopy of Graphene-based Materials and its Applications in Related Devices. *Chem. Soc. Rev*., 2018, **47**, 1822-1873. [CrossRef]
24 Shimodaira N.; Masui A. Raman Spectroscopic Investigations of Activated Carbon Materials. *J. Appl. Phys*., 2002, **92**, 902-909. [CrossRef]
25 Gopiraman M.; Babu S.G.; Khatri Z.; Wei K.; Endo M.; Karvembu R.; Kim I.S. Facile and Homogeneous Decoration of RuO_2 Nanorods on Graphene Nanoplatelets for Transfer Hydrogenation of Carbonyl Compounds. *Catal. Sci. Technol*., 2013, **3**, 1485-1489. [CrossRef]
26 Hulicova Jurcakova D.; Seredych M.; Lu G.Q.; Bandosz T.J. Combined Effect of Nitrogen-and Oxygen-Containing Functional Groups of Microporous Activated Carbon on its Electrochemical Performance in Supercapacitors. *Adv. Funct. Mater*., 2009, **19**, 438-447. [CrossRef]
27 Li Y.; Zhao Y.; Cheng H.; Hu Y.; Shi G.; Dai L.; Qu L. Nitrogen-Doped Graphene Quantum Dots with Oxygen-Rich Functional Groups. *J. Am. Chem. Soc*., 2011, **134**, 15-18. [CrossRef]
28 Gopiraman M.; Babu S.G.; Khatri Z.; Kai W.; Kim Y.A.; Endo M.; Karvembu R.; Kim I.S. An Eficient, Reusable Copper-Oxide/Carbon-Nanotube Catalyst for N-Arylation of Imidazole. *Carbon*, 2013, **62**, 135-148. [CrossRef]
29 Gopiraman M.; Bang H.; Babu S.G.; Wei K.; Karvembu R.; Kim I.S. Catalytic N-oxidation of Tertiary Amines on RuO_2 NPs Anchored Graphene Nanoplatelets. *Catal. Sci. Technol*., 2014, **4**, 2099-2106. [CrossRef]